

## Longitudinal beam dynamics in the Frascati DAΦNE $e^+e^-$ collider with a passive third harmonic cavity in the lengthening regime

David Alesini, Alessandro Gallo, Susanna Guiducci, Fabio Marcellini, and Mikhail Zobov  
*INFN Laboratori Nazionali di Frascati, P.O. Box 13, I-00044, Frascati (Roma), Italy*

Mauro Migliorati and Luigi Palumbo  
*INFN Laboratori Nazionali di Frascati, P.O. Box 13, I-00044, Frascati (Roma), Italy*  
*and Department Energetica, University "La Sapienza," Via Antonio Scarpa 14, I-00161 Roma, Italy*  
 (Received 3 February 2003; published 8 July 2003)

A high-harmonic rf system is going to be installed in both rings of the DAΦNE Φ-Factory collider to improve the Touschek lifetime. The main goal of this paper is to study the impact of the 3rd harmonic cavity on beam dynamics making a special emphasis on the dynamics of a bunch train with a gap. The shift of the coherent synchrotron frequencies of the coupled-bunch modes has been estimated. In the following we investigated the effect of magnification of the synchrotron phase spread and beam spectrum variation due to the gap. Besides we simulated the bunch lengthening for different bunches along the unevenly filled train and evaluated the Touschek lifetime enhancement taking into account the obtained bunch distributions. Finally, the "cavity parking" option is discussed. It can be considered as a reliable backup procedure consisting of tuning the cavity away from the 3rd harmonic frequency and in between two revolution harmonics. It allows recovering, approximately, the same operating conditions as were before the harmonic cavity installation.

DOI: 10.1103/PhysRevSTAB.6.074401

PACS numbers: 29.27.Bd, 29.20.Dh, 41.85.Ew, 41.75.Ht

### I. INTRODUCTION

The Frascati Φ-Factory DAΦNE [1] is a double ring, high luminosity collider working at the energy of the Φ-meson resonance (1.02 GeV in the center of mass). The most relevant DAΦNE parameters for luminosity delivery to the KLOE experiment (runs of year 2002) are summarized in Table I.

For low energy and high bunch current storage rings the beam lifetime is dominated by the Touschek scattering process [2]. Because of a scattering effect two particles performing transverse betatron oscillations inside the bunch can transform their transverse momenta into longitudinal ones. If the new longitudinal momenta are outside the momentum acceptance of the machine, the particles are lost. The resulting beam lifetime is inversely proportional to the number of particles in the bunch [3].

The Touschek effect is particularly harmful in DAΦNE because of the low beam energy and the large bunch charge density necessary to get the required luminosity. This effect leads to the production of beam induced background and the necessity of frequent beam injections because of the low beam lifetime. Increasing the DAΦNE beam lifetime is therefore one of the priorities in the machine performance upgrade activity.

The DAΦNE rf system can deliver a maximum accelerating voltage of  $\approx 300$  kV, which is more than twice the present operating rf voltages as reported in Table I.

However, we have found experimentally that the rf voltage increase is almost ineffective for the DAΦNE beam lifetime improvement since at voltages higher than  $\approx 150$  kV, the machine momentum acceptance is

presently limited by the small off-energy dynamic aperture. Moreover, increasing the rf voltage also decreases the natural bunch length, and, due to the high single-bunch current, this pushes further the machine operation in the microwave regime. As a matter of fact, we observed experimentally that the DAΦNE beam dynamics is more critical at higher rf voltages [4].

The strategy to improve the DAΦNE beam lifetime consists of three steps.

(i) To increase the off-energy dynamic aperture by improving the machine nonlinear model and, on its basis, to optimize the sextupole and octupoles setups. This study is well advanced [5].

(ii) To increase the energy acceptance by substantially increasing the rf peak voltage.

(iii) To lengthen the bunches at this high peak voltage of the main rf system by means of a high-harmonic voltage up to the limit imposed by the hourglass effect in beam-beam collisions.

We expect also that the last step will increase the single-bunch microwave instability threshold, since the natural bunch length with the harmonic voltage is higher.

According to the above strategy, a harmonic rf system based on a normal conducting, single-cell 3rd harmonic cavity powered by the beam (passive mode) has been designed and built and is going to be installed in both DAΦNE rings [6].

Studies, installations, and the operation of harmonic rf systems for storage rings for lifetime improvement are in progress also in a number of different laboratories [7–12].

There may be also other reasons for taking into consideration rf harmonic systems. For instance, the large

TABLE I. DAΦNE parameters (KLOE runs 2002).

Energy	$E$ (MeV)	510
Maximum beam current	$I_M$ (A)	1.2 (presently) 1.4–1.7 (goal)
Number of colliding bunches	$N_b$	47–51
Maximum current per bunch	$I_b$ (mA)	25 (presently) 30–35 (goal)
rf frequency	$f_{\text{rf}}$ (MHz)	368.29
rf voltage	$V_{\text{rf}}$ (kV)	100–150
Harmonic number	$h$	120
Bunch spacing	$T_b$ (ns)	5.43 (= $2/f_{\text{rf}}$ )
Synchrotron losses	$E_r$ (keV/turn)	9.3
Parasitic losses	$E_p$ (keV/turn)	$\approx 2.5$ (@ $I_b \approx 20$ mA, $e^-$ ring) $\approx 4.5$ (@ $I_b \approx 20$ mA, $e^+$ ring)
Momentum compaction	$\alpha_c$	$\approx 0.034$
Natural bunch length	$\sigma_{z0}$ (cm)	$\approx 1.6$ (@ $I_b \approx 0$ mA, $V_{\text{rf}} \approx 120$ kV)
Natural bunch energy spread	$\sigma_E/E$	$3.9 \times 10^{-4}$
Bunch length (lengthening regime)	$\sigma_z$ (cm)	$\approx 2.4$ ( $e^+$ , @ $I_b \approx 20$ mA, $V_{\text{rf}} \approx 120$ kV) $\approx 2.8$ ( $e^-$ , @ $I_b \approx 20$ mA, $V_{\text{rf}} \approx 120$ kV)
Vertical to horizontal emittance coupling	$\kappa = \varepsilon_y/\varepsilon_x$	$\approx 0.2\%$
Vertical beta function @ IP	$\beta_y^*$ (cm)	$\approx 3$
rf acceptance	$\varepsilon_{\text{rf}}/E$	$\approx 0.55\%$ (@ $V_{\text{rf}} \approx 120$ kV)
Beam lifetime	$\tau_T$ (s)	$\approx 1000$ – $2000$

nonlinear term introduced in the longitudinal machine dynamics tends to weaken the coherent effects through the Landau damping mechanism and may be therefore beneficial to both the single and coupled-bunch dynamics.

The use of rf harmonic systems in the shortening regime has been also suggested for luminosity upgrade of the existing “factory” colliders [13]. In this case ultra-low  $\beta$  insertions in the interaction regions are required, and this calls for very short bunches. The use of harmonic voltages to increase the total rf slope over the bunch may help to meet this requirement.

However, the harmonic voltage also perturbs other aspects of the longitudinal dynamics and may affect the beam stability and overall storage ring performance.

In the present paper we discuss the expected performance of the system and evaluate its impact on the longitudinal beam dynamics. Particular attention is given to multibunch dynamics of beams with bunch patterns with a gap to avoid ion trapping in the electron ring.

The paper is structured as follows. The choice of the design parameters of the DAΦNE rf harmonic system is discussed in Sec. II. Section III gives a detailed analysis of the most relevant beam dynamics aspects. In particular, in Sec. IIIA the shift of the coherent synchrotron frequencies of the coupled-bunch (CB) modes for a uniform filling pattern is calculated, which may lead to a destructive instability whenever any of them approaches zero. The spread of the synchronous phases for the operation with a gap in the beam filling pattern is calculated and discussed in Sec. IIIB, while the results of bunch

lengthening simulations for different bunches along the train are given in Sec. IIIC. The presence of a gap in the bunch filling pattern produces a large spread in parasitic losses and synchronous phases. As a consequence, the Touschek lifetime gain is not uniform over the train; different bunches will collide at different interaction points (IPs) and the synchronization of the bunch-by-bunch feedback systems may be affected.

Evaluation of the ultimate expected performances in terms of Touschek lifetime improvement is reported in Sec. IV, taking into account the simulated bunch length. The so-called “parking option,” consisting of tuning the cavity away from the 3rd harmonic frequency and in between two revolution harmonics, is considered and illustrated in Sec. V.

## II. RF CONFIGURATION FOR LIFETIME IMPROVEMENT

The Touschek lifetime can be improved by using the harmonic voltage to lengthen the bunch and/or by increasing the rf voltage to enlarge the energy acceptance [14].

In DAΦNE the bunch length depends on the bunch current (lengthening process), due to the interaction with the machine short-range wakefields (i.e., the machine broad-band impedance) [15]. Presently, as reported in Table I, the bunch lengths at typical operating conditions are 2.4 and 2.8 cm in the  $e^+$  and the  $e^-$  rings, respectively. The bunch length difference between the

two rings is explained by the higher broad-band impedance in the  $e^-$  ring due to the presence of ion clearing electrodes. A model of the DAΦNE short-range wakefields not including the contribution of the ion clearing electrodes predicts with good accuracy the lengthening process in the  $e^+$  ring [16].

In the near future the typical current per bunch in operation should be increased from 20–25 mA (present values) to 30–35 mA, in order to increase machine luminosity. Single-bunch measurements already performed on the two rings at the present operational rf voltage ( $\approx 120$  kV) show that the bunch lengths at 35 mA are  $\approx 2.8$  and 3.3 cm in the  $e^+$  and the  $e^-$  rings, respectively. These values are already at the limit allowed by the present value of the vertical  $\beta$  function at the IP (hourglass effect). This means that, with the present machine setup, there is no chance of lengthening further the bunch without affecting machine luminosity.

Therefore, the only possible strategy to improve the lifetime is based on the energy acceptance increase, which can be obtained by increasing the peak voltage of the main rf system. In this case the harmonic voltage is used to reduce the total rf slope at the bunch center in order to keep the bunch length near the hourglass limit.

A possible choice of the parameters of both main and harmonic rf systems based on the previous considerations is shown in Table II.

The 3rd harmonic of the main rf frequency has been chosen as a working frequency of the DAΦNE harmonic cavity as a good trade-off between efficiency and compactness requirements.

Since a very moderate harmonic voltage is required ( $V_H \approx 56$  kV), while the stored multibunch current in operation is quite large (already in the 1 A range and hopefully higher in the near future), it is straightforward to generate the harmonic voltage from the passive beam excitation of one cavity per ring. The passive option is far less complicated and expensive compared to the active one, and it does not present major drawbacks from the beam dynamics point of view. The optimization of the accelerating mode shunt impedance is not mandatory in

this case, and the cavity design has been mainly aimed at higher order modes (HOM) suppression. The DAΦNE harmonic cavity design, construction, and test activities are reported elsewhere [6]. The shunt impedance of this cavity is quite low ( $\approx 480$  k $\Omega$ ). This will require extra rf power to the main rf system, which is not an issue in our case. On the other hand, the lower the shunt impedance is, the weaker the coherent effects are.

In the following we will assume that the harmonic cavity is properly tuned between the revolution harmonics  $3h$  and  $3h + 1$  to get the voltage at any operating value of the beam current. This means

$$\begin{aligned} V_H &= -I_{3h}Z_H(3h\omega_0) = \frac{-I_{3h}R_H}{1 + jQ_H\delta_H} \Rightarrow |V_H| \\ &= |I_{3h}| \frac{R_H}{\sqrt{1 + (Q_H\delta_H)^2}}, \end{aligned} \quad (1)$$

$$\begin{aligned} \varphi_H &= \angle V_H \\ &= -\pi - \arctan(Q_H\delta_H) = -\frac{\pi}{2} + \arctan\left(\frac{1}{Q_H\delta_H}\right), \end{aligned} \quad (2)$$

where  $I_{3h}$  is the  $3h$  line of the unilateral beam spectrum,  $Z_H$  is the harmonic cavity impedance, and  $\delta_H = 3h\omega_r/\omega_H - \omega_H/(3h\omega_r)$  is the harmonic cavity detuning parameter ( $\omega_H$  being the resonant angular frequency of the harmonic cavity and  $\omega_r$  the revolution angular frequency). This harmonic voltage can be obtained at various operating currents by setting the cavity detuning according to

$$Q_H\delta_H = -\sqrt{\left(\frac{|I_{3h}|R_H}{|V_H|}\right)^2 - 1}. \quad (3)$$

Tuning the cavity above the  $3h$  revolution harmonic (i.e., negative values of the  $\delta_H$  parameter) provides the right phasing with respect to the main rf voltage to lengthen the bunches. One may also notice that for typical operating currents ( $I \approx 1$  A), the absolute value of the  $Q_H\delta_H$  product is larger than 10. This means that the impedance

TABLE II. Proposed DAΦNE rf parameter set.

Main rf voltage	$V_{\text{rf}}$ (kV)	200
Main cavity shunt impedance	$R_s = V^2/2P_{\text{rf}}$ (M $\Omega$ )	1.9
Main cavity $Q$ factor	$Q_0$	31 500
Main cavity input coupling factor	$\beta$	$\approx 4.6$
rf harmonic frequency	$f_H$ (MHz)	1104.87 = $3f_{\text{rf}}$
rf harmonic voltage	$V_H$ (kV)	56
Harmonic cavity shunt impedance	$R_H = V^2/2P_H$ (M $\Omega$ )	0.48
Harmonic cavity $Q$ factor	$Q_{0_H}$	18 500
Natural bunch length	$\sigma_{z0}$ (cm)	$\approx 2.5$ (@ $I_b \approx 0$ mA)
Bunch length (lengthening regime)	$\sigma_z$ (cm)	$\approx 3.1$ (@ $I_b \approx 35$ mA)
rf acceptance	$\varepsilon_{\text{rf}}/E$	$\approx 0.7\%$

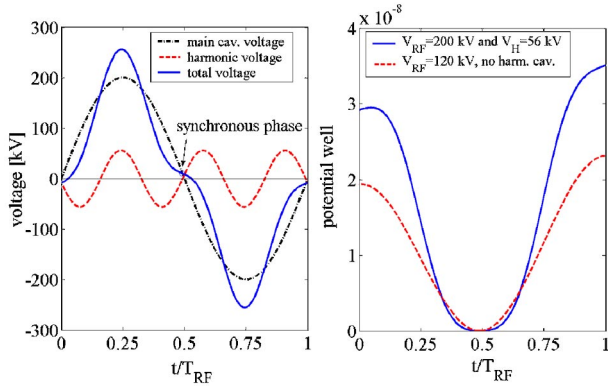


FIG. 1. (Color) Total rf voltage and potential well.

of the harmonic cavity sampled at the 3rd harmonic frequency  $Z_H(3h\omega_r)$  is mainly reactive and produces a harmonic voltage that is almost completely out of phase with respect to the beam. Plots of the main and harmonic voltages and their sum, together with the resulting potential well, are shown in Fig. 1 at  $Q_H\delta_H = -25$ .

The “natural” and “lengthened” bunch profiles over the total rf voltage are shown in Fig. 2. The natural bunch profile is obtained by solving the Haissinski equation [17] neglecting the machine short-range wakefields. The lengthened profile is obtained from a multiparticle tracking simulation that includes the wakefields [18].

$$(\omega_c/\omega_i)_n^2 = 1 + \frac{2I\alpha_c}{\omega_i^2 2\pi h E/e} \sum_{p=iN_b \pm n \pm \nu_c} p Z_i(p\omega_r) e^{-(p\omega_r\sigma_i)^2}; \quad i = \text{any integer}, \quad (4)$$

where  $E/e$  is the beam energy in eV units,  $\nu_c = \omega_c/\omega_r$  is the coherent synchrotron tune,  $\sigma_i$  is the rms bunch length in time units,  $Z_i$  is the imaginary part of the machine impedance, while  $\omega_i$  is the incoherent synchrotron angu-

lar frequency and is given by

### III. BEAM DYNAMICS WITH THE HARMONIC CAVITY

#### A. Shift of the coherent synchrotron frequencies of the coupled-bunch modes (uniform filling pattern)

In conclusion, the proposed rf working point should provide a bunch length close to the hourglass limit, with an energy acceptance  $\approx 30\%$  higher with respect to the present DAΦNE operating conditions. In addition, since the harmonic voltage makes the natural bunch length much larger, the lengthening process is less pronounced, which indicates that microwave effects and single-bunch dynamics are relaxed.

lar frequency and is given by

$$\omega_i^2 = \omega_{\text{rf}}^2 \alpha_c \frac{V_{\text{rf}} \sin \varphi_s - 3V_H \sin \varphi_H}{2\pi h E/e}. \quad (5)$$

In the previous expression for  $\omega_i$  the contribution of the harmonic voltage is already included, and  $\omega_i$  is the frequency of the synchrotron oscillations of particles at small amplitudes in the potential well due to the combination of main and harmonic voltages.

The shift of the coherent frequency of the CB modes is due to the interaction between the beam spectrum sidebands of the bunch coherent motion and the imaginary part of the machine impedance. In our calculations we consider only the contribution of the accelerating modes of the main and harmonic cavities to the machine impedance. As shown in Fig. 3, the most affected coupled-bunch modes are those having their sidebands close to the resonant frequencies of the main and harmonic cavity accelerating modes, that is CB modes “0,” “1,” and “ $N_b - 1$ .” The ratio between coherent and incoherent values of the synchrotron frequencies for modes 0, 1, and  $N_b - 1$  as a function of the stored current is shown in Fig. 4. The mode 0 is the most perturbed one, since it interacts with the impedance of both main and harmonic

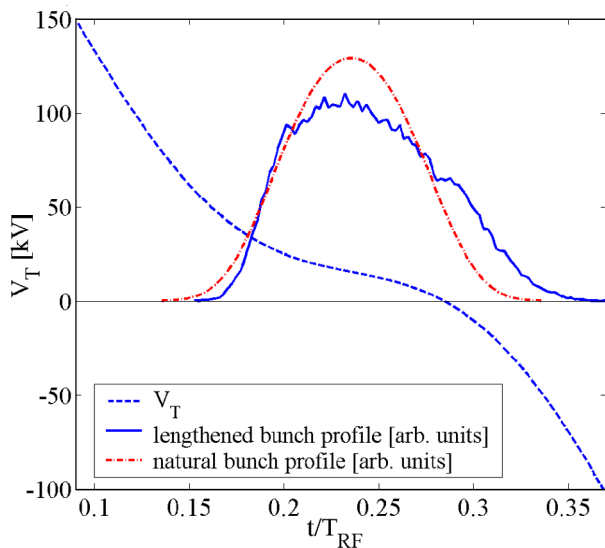


FIG. 2. (Color) Bunch profiles.

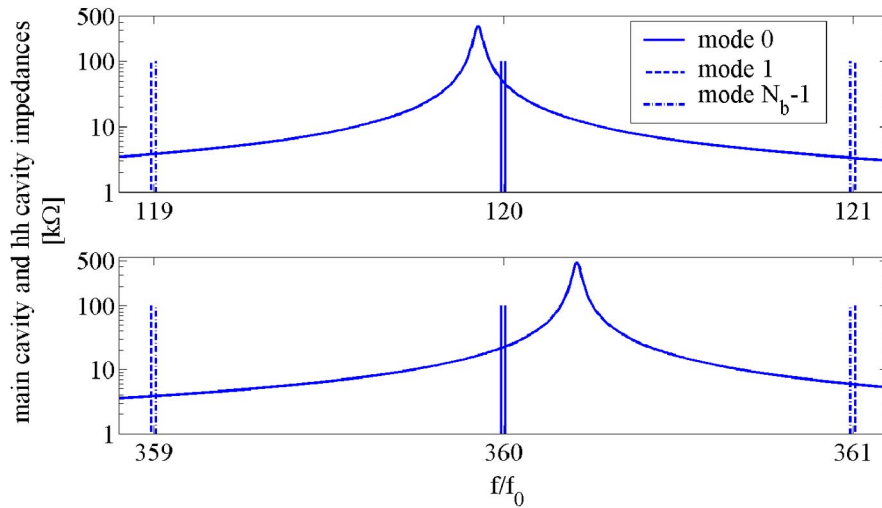


FIG. 3. (Color) Cavity impedances and CB mode sidebands.

cavities and, if its coherent frequency becomes too small, the beam can become unstable (2nd Robinson limit). To avoid this a large detuning of the main rf cavity must be provided ( $\varphi_z \approx 50^\circ$ ), and this condition corresponds to an inefficient operation of the main rf system ( $\approx 60\%$  of rf power reflected at the cavity input coupler). However, this is a conservative estimate since it is based on a linear theory and the effects of the large nonlinearity of the longitudinal focusing force are not taken into account.

The problem of the mode 0 coherent frequency shift can be relaxed by implementing a direct rf feedback around the rf system [21] that reduces the imaginary impedance sampled by the mode 0 sidebands and, as consequence, the shift of the mode 0 coherent frequency. The expected shift of the coherent frequencies of modes 1

and  $N_b - 1$  is much smaller, while it is almost negligible for the other coupled-bunch modes. With the exception of mode 0, which is damped by a dedicated feedback system as well as by the Robinson mechanism, the frequencies of all the CB modes remain inside the operational bandwidth of the DAΦNE bunch-by-bunch longitudinal feedback system (LFB system) [22] that keeps the beam stable in the longitudinal plane.

Damping rates of modes 0 and  $N_b - 1$  and the growth rate of mode 1 coming from the interaction between coherent sidebands of the coupled-bunch modes and the impedances of the accelerating modes of both the main and the harmonic cavities are shown in Fig. 5. The expected growth rate of mode 1 is much smaller than the typical damping rate provided by the DAΦNE LFB system ( $\approx 10 \text{ ms}^{-1}$ ).

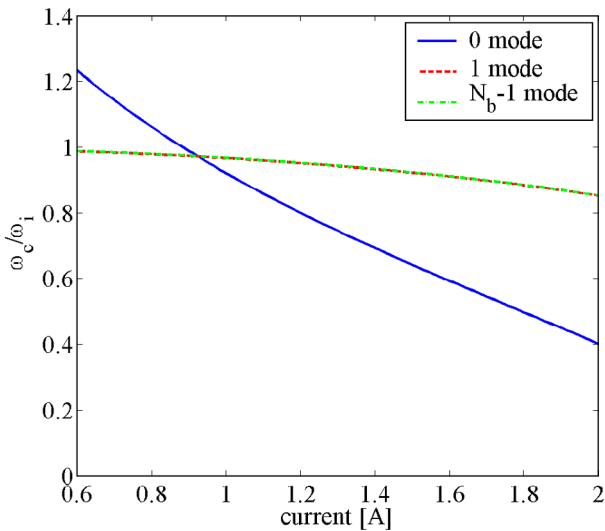


FIG. 4. (Color) CB modes frequency shift.

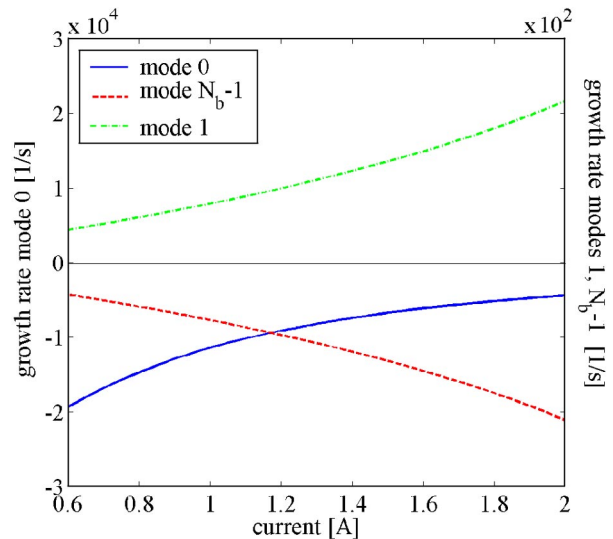


FIG. 5. (Color) CB modes growth and damping rates.

## B. Operation with a gap in the bunch filling pattern: spread of the synchronous phases

The modal expansion which is the base of the theory used in the previous paragraph to calculate the coherent frequency shifts is completely appropriate only in the case of multibunch beams with uniform filling pattern (same charge and shape of each bunch and no gaps along the pattern). This condition cannot be fulfilled in DAΦNE, since a gap of 15%–25% in the filling pattern is required in the  $e^-$  ring to prevent ion trapping. The analytic results obtained from the theory must be interpreted as an indication and have to be validated by numerical simulations.

A multibunch tracking code to study the machine longitudinal dynamics has been developed since the very early phase of the DAΦNE machine design and continuously upgraded through the years [23]. The bunches are modeled as macroparticles and tracked turn by turn in the longitudinal phase space including the following:

- (i) Basic features of the machine lattice, such as momentum compaction factor and radiation damping.
- (ii) Narrow-band machine impedances, in terms of a set of resonant modes, each identified by its resonant frequency, impedance, and  $Q$  factor.
- (iii) LFB system, including realistic models for the front-end, digital filtering, and back-end hardware.
- (iv) Main rf cavity, including a realistic model of the whole rf system and feedbacks.

The passive harmonic cavity is modeled just as a peculiar narrow-band impedance of the machine.

Results from tracking simulations of uniformly filled multibunch beams are in very good agreement with the theory. However, when a gap is introduced in the bunch filling pattern, the situation described by the tracking code is strongly perturbed. In the presence of a gap a head and a tail of the bunch train can be identified. The long-range wakes sampled by each bunch depend on the bunch position along the train. This generates a spread of the parasitic losses along the train and, as consequence, a spread of the synchronous phases of the bunches. This effect is already evident in DAΦNE, but, due to the large linear range of the rf voltage, it does not significantly affect the synchrotron frequency and the shape of each bunch.

The effect is largely magnified by the harmonic voltage. In this case the long-range wakes include the contribution due to the harmonic cavity accelerating impedance, and the parasitic loss spread increases. But the total rf voltage (main cavity + harmonic cavity) has very little slope around the synchronous phase and is also strongly nonlinear. The result is that the parasitic loss spread is converted in a large synchronous phase spread.

This effect can be also conveniently described in the frequency domain. Because of the gap in the filling pattern, the beam spectrum contains all the revolution har-

monics, and the beam current can be expressed by its Fourier expansion:

$$i(t) = \text{Re} \left( \sum_{k=0}^{+\infty} I_k e^{jk\omega_r t} \right). \quad (6)$$

In the ideal case, with no gap in the pattern, only the harmonics of the bunch repetition frequency (“powerful” harmonics) would be present ( $k = ihT_{\text{rf}}/T_b$ ,  $i$  any integer). Actually, because of the gap, the other lines are also present, and the total accelerating voltage is given by

$$V_T(t) = V_{\text{rf}} \cos(\omega_{\text{rf}} t + \varphi_s) + V_H \cos(3\omega_{\text{rf}} t + \varphi_H) + V_{NH}(t), \quad (7)$$

with

$$V_{NH}(t) = \text{Re} \left( - \sum_{k \neq h, 3h} I_k Z(k\omega_r) e^{jk\omega_r t} \right), \quad (8)$$

where  $Z(\omega)$  is the ring impedance, which is mainly given by the two narrow-band contributions of the rf cavity and harmonic cavity accelerating modes. In the previous expression the total voltage  $V_T(t)$  is represented as a sum of three terms. The first one is the main rf voltage, which is actively excited by the rf system; the second term is the harmonic voltage, which is passively excited by the beam with an amplitude that can be varied by changing the harmonic cavity tuning. The third term  $V_{NH}(t)$ , contrary to the previous two, has only the revolution periodicity, which means that it produces a constant voltage over a given bunch, but different voltages over different bunches in the train. We indicate this term as the “nonharmonic” voltage, and the parasitic loss spread is the spread of the nonharmonic voltage values as sampled by the bunches along the train.

Results of the tracking simulation comparing the present DAΦNE working point to the one proposed for implementing the harmonic cavity are shown in Fig. 6. In these simulations a train of 47 bunches spaced by two rf periods with a gap of  $\approx 22\%$  with a total current of 1.2 A is considered. The long-range wakes in the simulations are generated only by the accelerating modes of the main and harmonic cavities. In Fig. 6 dots represent the positions of the macroparticles distributed over the sum of the main and harmonic voltages. It may be seen that the spread of parasitic losses and synchronous phases grow by a factor of  $\approx 2.4$  and  $\approx 5.8$ , respectively, when the harmonic cavity is inserted.

The synchronous phase as a function of the bunch number for a train of 47 bunches spaced by two rf periods, including the effect of the harmonic cavity, and for total current values of 0.8, 1.2, 1.6, and 2 A are shown in Fig. 7. The synchronous phase variation is almost linear along the train and varies from  $\approx 180$  to  $\approx 320$  ps, accordingly to our multibunch tracking simulations.

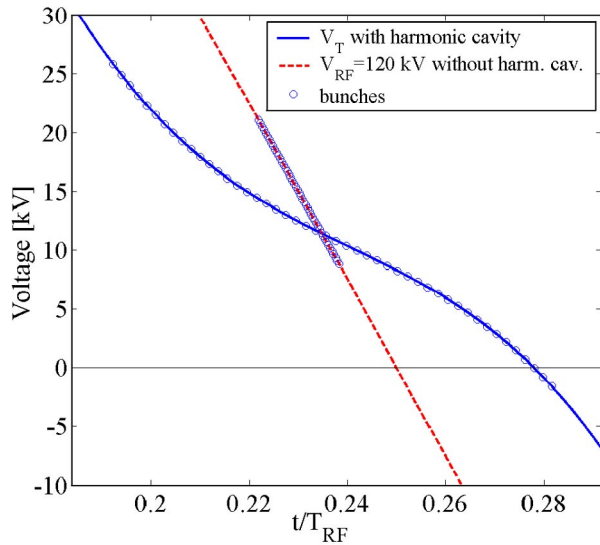


FIG. 6. (Color) Bunch position over the rf voltage.

It is also noticeable that the displacement of the bunch positions from a common synchronous value produces a significant distortion of the beam current spectrum. As an example, the spectra of the macroparticle beam current in the two cases reported in Fig. 6 are compared in Fig. 8. Since the basic bunch spacing is obtained by filling every other bucket, the beam spectrum peaks around the frequencies  $nf_{rf}/2$  (powerful harmonics).

A large head-tail displacement of the bunch synchronous phases produces a modulation of the powerful harmonics and a distortion of the revolution harmonics around them. It was surprising to find that in this case the intensity of the line  $3h$  (the beam spectrum line powering the 3rd harmonic cavity) is comparable with that of the adjacent line  $(3h + 1)$ . It is worth mentioning

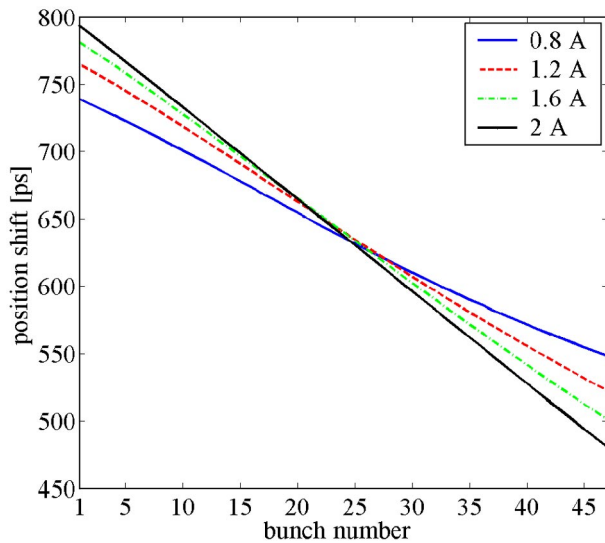


FIG. 7. (Color) Synchronous phase spread for various currents.

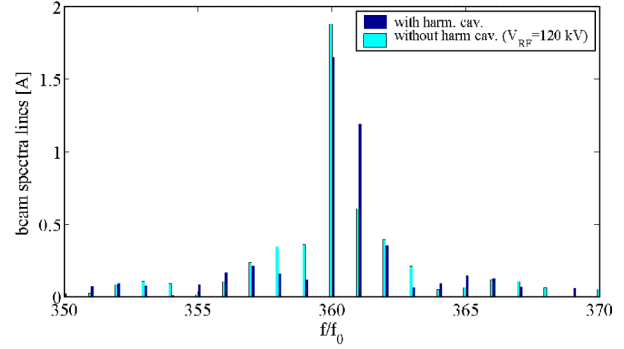


FIG. 8. (Color) Spectra of the beam with a gap in the filling pattern.

that, as long as the phase variation along the train is almost linear, a simple expression to compute the amplitude of the beam spectrum lines can be used. In this case we can assume that the time delay  $\Delta T_n$  of the  $n$ th bunch of the train ( $0 \leq n \leq N_b - 1$ ,  $N_b$  total number of bunches) with respect to the main rf voltage is given by

$$\Delta T_n = \Delta T_0 + n\Delta T, \quad (9)$$

and the amplitude of the  $k$ th line of the beam spectrum is given by

$$I_k = I \frac{\sin[kN_b/2(2\pi m/h + \omega_r \Delta T)]}{N_b \sin[k/2(2\pi m/h + \omega_r \Delta T)]} e^{-(k\omega_r \sigma_t)^2/2}, \quad (10)$$

where  $I$  is the total beam current,  $m = T_b/T_{rf}$  is the ratio between the bunch spacing and the rf period, and  $\sigma_t$  is the rms bunch length in time units.

The total voltage and the nonharmonic voltage around bunches 1, 12, 24, 36, and 47 are plotted in Fig. 9 for a beam of 1.6 A in 47 bunches. The nonharmonic voltage sampled at the position of the bunch centroid sets the bunch parasitic loss individual value. The shape of the nonharmonic voltage over the bunch is an additional perturbation of the potential well that has to be taken into account to compute the bunch natural and lengthened profiles. In particular, it may be observed that the bunches at the edge of the train seat close to maxima or minima of the nonharmonic voltage and their potential well are almost unperturbed. On the contrary, the phase of the nonharmonic voltage is almost opposite to that of the 3rd harmonic voltage over the central bunches of the train, so that the lengthening effect is weakened.

### C. Lengthening of bunches along the train

Since the bunch centroids occupy different positions along the total rf voltage (which is largely nonlinear) and since the nonharmonic voltage has a different form over the bunches, each bunch seats at a different rf slope and ends up with its own synchrotron frequency and charge distribution. So, each bunch has its own natural length, its

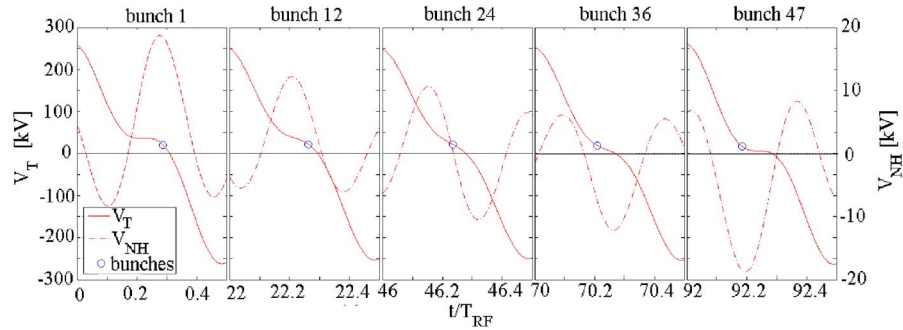


FIG. 9. (Color) Total voltage and the nonharmonic voltage on the bunches along the train with a gap.

equilibrium profile (in the lengthening regime) thus defining its own Touschek lifetime.

The natural and lengthened profiles of bunches 1, 12, 24, 36, and 47 are shown in Fig. 10 calculated for a beam of 1.6 A distributed over 47 bunches ( $\approx 34$  mA per bunch). The positions of the bunch centroids have been obtained from the macroparticle tracking, while the profiles have been obtained from the multiparticle tracking. The rms bunch length and the incoherent synchrotron frequency as a function of bunch number are reported in Fig. 11 for the beam parameters of Fig. 10. It may be seen that the bunches in the central part of the train do not reach the design length. This is because the rf slope over the central bunches is increased by the nonharmonic voltage contribution.

A large spread of the synchronous phases is cumbersome at least from two points of view. First of all, the position of the IP changes from bunch to bunch which may cause problems to the experiments as well as luminosity degradation if some bunch centroids collide significantly apart from the waist of the vertical  $\beta$  function. One could argue that, provided the synchronous phase spread is equal in the two beams, the IP positions remain fixed and only the collision times vary with respect to the rf clock. But there is little hope that the synchronous

phase spread will be equal in the two rings, since in each ring it is generated by the long-range wakefields associated with all machine HOMs. As a matter of fact, we already observed a substantial difference in the bunch phase spread between the two rings in the present operation, which is probably due to a difference in the HOM distribution in the two  $e^+$  and  $e^-$  ring rf cavities (whose internal profile is not exactly equal).

The impact of the bunch phase spread on the operational efficiency of the DAΦNE LFB system is the second worrying aspect. The LFB is a synchronous system timed on the rf clock. In particular, the front end works at  $6f_{\text{rf}}$ , while the back end (the part of the hardware dedicated to properly kick each bunch) works at  $3.25f_{\text{rf}}$ . Both hardware sections will suffer from an excessive phase deviation of the bunch from a common equilibrium value. In particular, the front-end phase detector has only a limited dynamic range, which can be spoiled by an excessive phase spread, while the back-end section cannot be properly phased on all the bunches.

The tracked oscillations of bunches 1, 24, and 47 for a beam current of 1.6 A distributed over 47 bunches (every other bucket filling) with and without LFB are shown in Fig. 12. It may be seen that the damping of the LFB is still necessary, even though we know that it cannot be

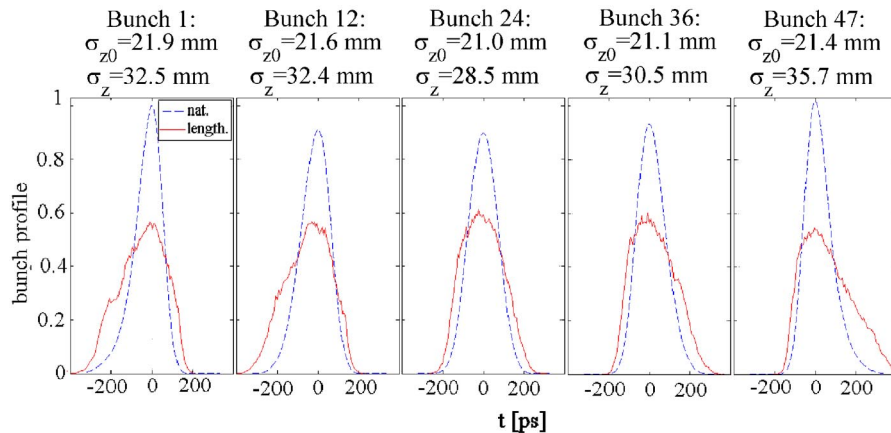


FIG. 10. (Color) Natural and lengthened profiles of the bunches along the train with a gap.

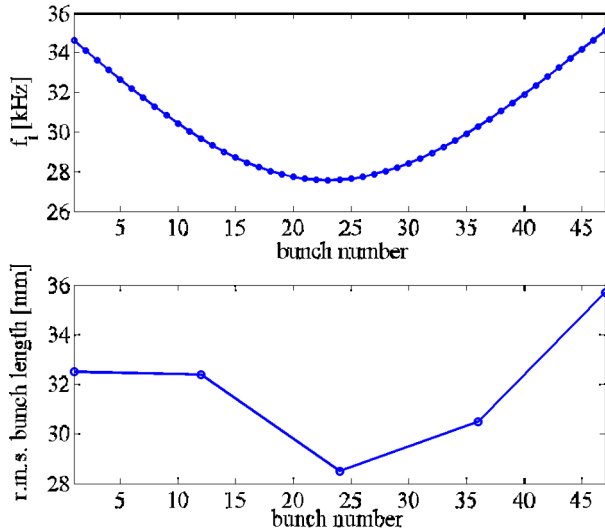


FIG. 11. (Color) rms bunch length and bunch incoherent synchrotron frequency along the train.

effective on the bunches near the train edges because of the off time of both the front-end and back-end sections. In this case the beam is kept stable by the cooperation of LFB and Landau damping.

It might be asked whether there is a way to limit the spread of the synchronous phases or, at least, some of its effects. In the  $e^+$  ring only it is possible to remove the spread by removing the gap in the filling pattern. This will increase the average beam current, increasing the background production but not the luminosity, since the extra bunches closing the gap have no “partner” bunches in the other beam. Nevertheless, this kind of operation may have some advantages like a better average lifetime of the  $e^+$  beam and a less critical operation of the  $e^+$  LFB system.

The criticality of the LFB system operation could be possibly reduced even without removing the gap. In this case one should, in principle, synchronize the system on a linearly phase modulated rf tone, to follow the phase displacement from bunch to bunch. A solution of this kind seems to be feasible from a technical point of view.

#### IV. EXPECTED IMPROVEMENT IN TOUSCHEK LIFETIME WITH THE 3RD HARMONIC CAVITY

The beam lifetime due to Touschek scattering has been calculated in Gaussian bunch approximation assuming that the limiting acceptance for the relative momentum deviation is given by the minimum between the rf acceptance and the transverse physical aperture of the machine [24]. The limitations coming from the finite dynamic aperture are not included in these calculations.

The estimated lifetimes are plotted in Fig. 13. In the plot the bunch lifetimes with the harmonic cavity are normalized to those calculated in the present operation conditions ( $V_{\text{rf}} = 110$  kV) and with  $V_{\text{rf}} = 200$  kV (without harmonic cavity) for two different bunch currents (17 and 34 mA). Considering the cases with no gap, it is important to observe the following:

- (i) All bunches have the same lifetime because they have the same charge distribution.
- (ii) There is an improvement of  $\approx 90\%$  and  $\approx 75\%$  in the lifetime with a bunch current of 17 and 34 mA, respectively. This improvement is given by the enlargement of the energy acceptance and by the fact that the bunch is longer.
- (iii) In the case of 34 mA/bunch the improvement is reduced because the lengthening process without the harmonic cavity is more pronounced.

In the presence of a gap, because of the different charge distributions, each bunch has its own lifetime. Also in this case, however, the average beam lifetime improvement is

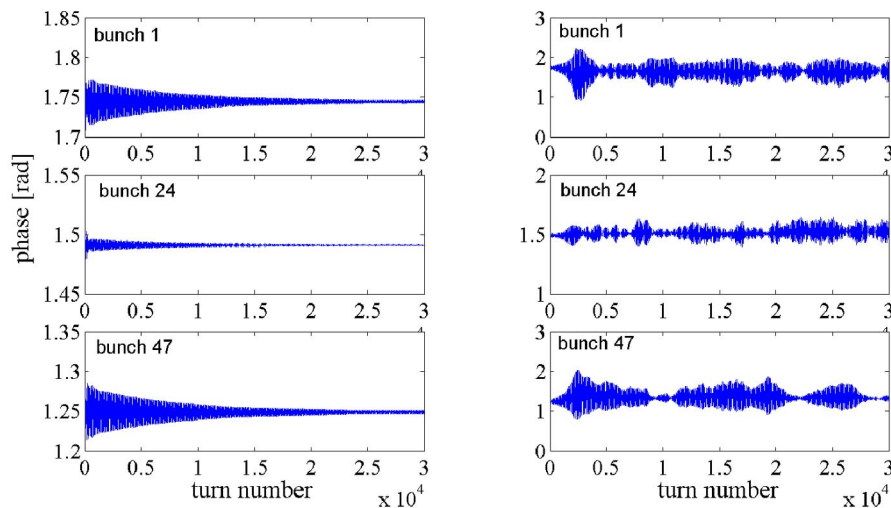


FIG. 12. (Color) Tracked oscillations of bunches ( $I_b = 1.6$  A into 47 bunches) with LFB on and off.

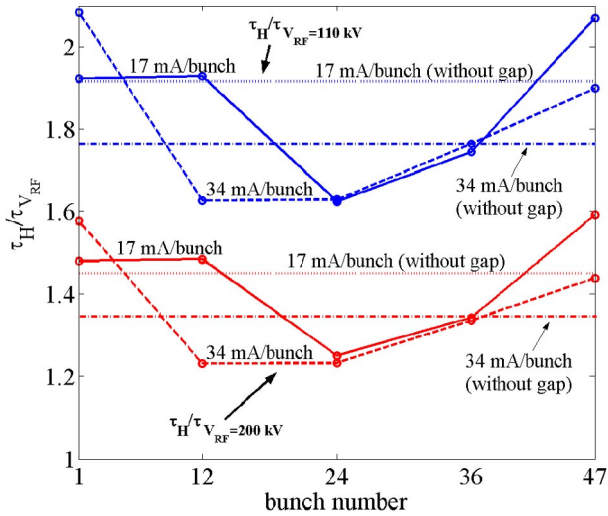


FIG. 13. (Color) DAΦNE Touschek lifetime improvement with the harmonic cavity.

$\approx 80\%$  and is lower for the central bunches of the train that are shorter.

Similar considerations can be done in the case of  $V_{rf} = 200$  kV. In this case the improvement is given only by the fact that the bunch is longer because the energy acceptance is almost the same ( $\approx 0.75\%$ ).

The computed lifetime improvements do not take into account the limitations in the momentum acceptance coming from the dynamic aperture. From this point of view, the computed improvements have to be assumed as limit values if the dynamic aperture could be increased at a level where it becomes not relevant in the Touschek process.

## V. THE CAVITY DETUNING (PARKING) OPTION

As discussed in the previous paragraphs, the implementation of the harmonic cavity presents beneficial aspects such as lifetime and Landau damping increase, but also produces other effects like the amplification of the synchronous phase spread, whose impact on the collider performance is not completely predictable. A backup procedure consists of tuning the harmonic cavity in between two revolution harmonics sufficiently away from the  $3h$  lines [for instance,  $\omega_H \approx (3h + \Delta n)\omega_r$ ,  $\Delta n = 1.5, 2.5,$  and  $3.5$ ]. This option is the so-called “cavity parking.” In this way the harmonic voltage is very low and the interaction of the cavity impedance with the beam is minimized (but still significant). By “parking” the harmonic cavity one expects to recover the operating conditions existing before the harmonic cavity installation. The plot of the coherent CB mode frequencies and of the incoherent synchrotron frequency vs the beam current for  $\Delta n = 2.5$  is reported in Fig. 14. It can be seen that the frequency shifts are small enough to consider the perturbation negligible. The synchronous phase

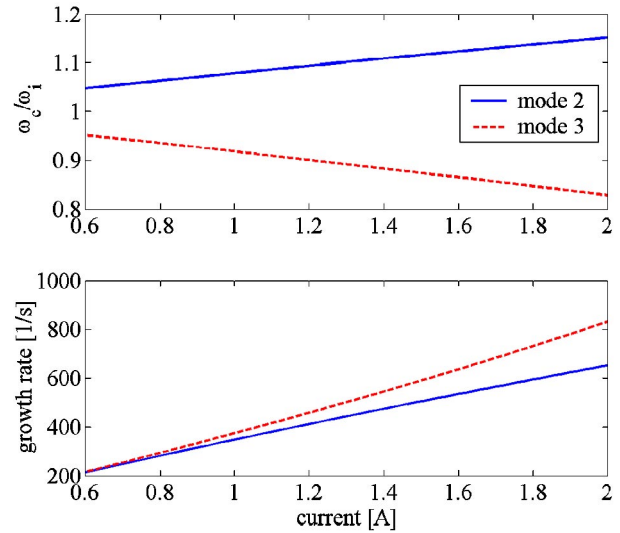


FIG. 14. (Color) Coherent CB mode frequencies and growth rates vs beam current,  $\Delta n = 2.5$ .

spread for a current of 1.6 A distributed over 47 bunches is shown in Fig. 15 for  $\Delta n = 1.5, 2.5,$  and  $3.5$ . It may be seen that the phase deviation is not linear anymore with the bunch position along the train, while the total spread is even smaller than the value expected at the same current without harmonic cavity. This is not surprising, since it may be demonstrated that, provided that  $|\Delta n| > 1$ , there is a partial compensation of the wakes generated by the accelerating mode impedances of the main and harmonic cavities.

## VI. CONCLUSIONS

The 3rd harmonic passive rf system will be installed in both collider rings of the  $\Phi$ -Factory DAΦNE to improve

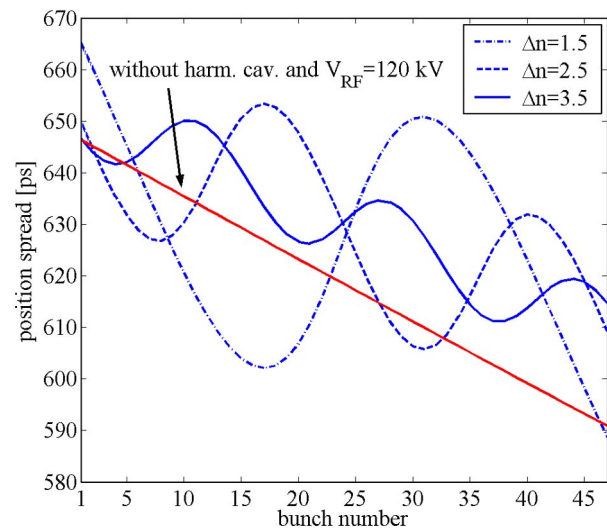


FIG. 15. (Color) Synchronous phase spread ( $I_b = 1.6$  A into 47 bunches) for various  $\Delta n$ .

the beam Touschek lifetime. For this purpose we plan to increase the energy acceptance of the machine by increasing the rf peak voltage and to lengthen the bunches at this high peak voltage by means of the harmonic voltage up to the limit imposed by the hourglass effect in beam-beam collisions.

We have evaluated that the use of the harmonic cavity in the lengthening regime can improve the Touschek lifetime of the DAΦNE beam up to  $\approx 80\%$  with respect to the present operating conditions. The simulations have shown that the microwave lengthening process is less pronounced in this case. Besides, we expect the enhancement of the Landau damping due to the large nonlinearity of the harmonic voltage which should relax the single and multibunch dynamics.

However, by analyzing the beam dynamics we have found that the harmonic system can introduce a few undesirable effects. The presence of a gap in the bunch filling pattern will produce a large spread in parasitic losses and synchronous phases (thus modifying also the beam spectrum). As a consequence, different bunches will collide at different IPs and the synchronization of the bunch-by-bunch feedback systems may be affected. Moreover, as we have seen in numerical simulations, the bunch charge distribution changes for different bunches along the train and the Touschek lifetime gain is not uniform over the train. The actual tolerability of such effects cannot be exactly predicted since it depends on the eventual operating conditions (such as the gap width, for example). That is why we have foreseen the “parking option” (consisting of tuning the cavity away from the 3rd harmonic frequency and in between two revolution harmonics) which allows recovering substantially the operating condition before the harmonic cavity installation and can be considered as a reliable backup procedure. Moreover, in the parking option the synchronous phase spread is compressed by a long-range wake compensation effect, and the very moderate harmonic voltage still present is expected to increase Landau damping in the longitudinal dynamics.

#### ACKNOWLEDGMENTS

The authors would like to thank R. Boni, M. Serio, and P. Raimondi for helpful discussions on the subject. Thanks also to A. Drago for his contribution to the understanding of the harmonic cavity impact on the longitudinal feedback system.

- [1] M. Zobov *et al.*, in *Proceedings of the 2002 European Particle Accelerator Conference, Paris* (EPS-IGA/CERN, Geneva, 2002), p. 443.
- [2] C. Bernardini *et al.*, *Phys. Rev. Lett.* **10**, 407 (1963).
- [3] H. Bruck, *Accélérateurs Circulaires de Particules* (Presses Universitaires de France, Paris, 1966).
- [4] A. Drago, in *Proceedings of the 2002 European Particle Accelerator Conference, Paris* (Ref. [1]), p. 239.
- [5] P. Raimondi (private communication).
- [6] A. Gallo *et al.*, in *Proceedings of the 2001 Particle Accelerator Conference, Chicago* (IEEE, Piscataway, NJ, 2001), p. 885.
- [7] J. M. Byrd, *et al.*, *Phys. Rev. ST Accel. Beams* **5**, 092001 (2002).
- [8] M. Svandrlík *et al.*, in *Proceedings of the 2000 European Particle Accelerator Conference, Vienna* (CERN, Geneva, 2000), p. 2052.
- [9] P. Marchand, in *Proceedings of the 1999 Particle Accelerator Conference, New York City* (IEEE, Piscataway, NJ, 1999), p. 989.
- [10] M. Georgsson *et al.*, in *Proceedings of the 2000 European Particle Accelerator Conference, Vienna* (Ref. [8]), p. 1960.
- [11] L. H. Chang *et al.*, in *Proceedings of the 1997 Particle Accelerator Conference, Vancouver* (IEEE, Piscataway, NJ, 1997), p. 1691.
- [12] A. Gallo *et al.*, in *Proceedings of the 2000 European Particle Accelerator Conference, Vienna* (Ref. [8]), p. 1495.
- [13] Y. Ho Chin, Berkeley Report No. LBL-29622, 1990.
- [14] M. Migliorati, L. Palumbo, and M. Zobov, *Nucl. Instrum. Methods Phys. Res., Sect. A* **354**, 215 (1995).
- [15] A. Ghigo *et al.*, in *Proceedings of the 2002 European Particle Accelerator Conference, Paris* (Ref. [1]), p. 1494.
- [16] A. Gallo *et al.*, in *Proceedings of the  $e^+e^-$  Factories '99 Workshop, KEK, Tsukuba* (KEK, Tsukuba, 2000), p. 105.
- [17] J. Haissinski, *Il Nuovo Cimento Soc. Ital. Fis.* **18B**, 72 (1973).
- [18] M. Zobov *et al.*, in *Proceedings of the International Workshop on Collective Effects and Impedance for B-Factories, Tsukuba* (KEK, Tsukuba, 1996), p. 110.
- [19] A. Hofmann, CERN Report No. 95-06, 1995, Vol. 1, p. 307.
- [20] J. L. Laclare, CERN Report No. 87-03, 1987, Vol. 1, p. 264.
- [21] D. Boussard, CERN Report No. 91-04, 1991, p. 294.
- [22] A. Drago *et al.*, in *Proceedings of the 2001 Particle Accelerator Conference, Chicago* (Ref. [6]), p. 3543.
- [23] S. Bartalucci *et al.*, *Part. Accel.* **48**, 213 (1995).
- [24] S. Guiducci, DAΦNE Technical Note No. L-12, Frascati, 1993.